Slovak University of Technology in Bratislava
Faculty of Civil Engineering

Ing. Martin Ambroz

Dissertation Thesis Abstract

Numerical modelling of the forest fire propagation

to obtain the Academic Title of *philosophiae doctor (PhD.)*
in the doctorate degree study programme
9.1.9 Applied Mathematics

Bratislava 2018

Dissertation Thesis has been prepared at Department of Mathematics and Descriptive Geometry, Faculty of Civil Engineering, Slovak University of Technology in Bratislava.

Submitter: Ing. Martin Ambroz
Department of Mathematics and Descriptive Geometry
Faculty of Civil Engineering, STU, Bratislava

Supervisor: prof. RNDr. Karol Mikula, DrSc.
Department of Mathematics and Descriptive Geometry
Faculty of Civil Engineering, STU, Bratislava

Readers: prof. RNDr. Daniel Ševčovič, DrSc.
Department of Applied Mathematics and Statistics
Faculty of Mathematics, Physics and Informatics, CU, Bratislava

doc. RNDr. Ladislav Halada, CSc.
Institute of Informatics
Slovak Academy of Sciences, Bratislava

doc. RNDr. Peter Frolkovič, PhD.
Department of Mathematics and Descriptive Geometry
Faculty of Civil Engineering, STU, Bratislava

Dissertation Thesis Abstract was sent ....

Dissertation Thesis Defence will be held on .... at .... am/pm at Department of Mathematics and Descriptive Geometry, Faculty of Civil Engineering, Slovak University of Technology in Bratislava, Radlinského 11.

prof. Ing. Stanislav Unčík, PhD.
Dean of Faculty of Civil Engineering

Abstrakt

V tejto dizertačnej práci predstavujeme nový model šírenia lesných požiarov. Náš prístup je založený na vývoji trojrozmernej krivky na ploche, ktorá predstavuje hranicu požiaru na topografii. Náš matematický model pre vývoj krivky je postavený na empirických zákonoch šírenia požiarov ovplyvnených palivom, vetrom, sklonom terénu a tvarom hranice požiaru s ohľadom na topografiu (geodetická a normálová krivosť). Táto krivka na ploche je projektovaná do horizontálnej roviny ako rovinná krivka, ktorej vývoj je riešený numericky a nová krivka je namapovaný naspäť na plochu. Pre numerické riešenie diskretizujeme vznikajúcu intrinsickú parciálnu diferenciálnu rovnicu. Pre krivostný člen používame semi-implicitnú schému a advekčný člen diskretizujeme pomocou tzv. inflow-implicit/outflow-explicit metódy a implicitnej upwind schémy, čo zabezpečí riešiteľnosť lineárneho systému efektívnym trojdiagonálnym riešičom bez časového obmedzenia a robustnosť vzhľadom na singularity. Naše rýchle riešenie pre detekciu topologických zmien (delenie a spájanie kriviek) je nielen popísané, ale aj vizualizované na konkrétnej situácii. Prezentujeme aj experimentálny rád konvergencie numerickej schémy, demonštrujeme vplyv parametrov modelu na šírenie požiaru na testovacej a reálnej topografii a rekonštruujeme simulovaný požiar trávnatého porastu.

Kľúčové slová: krivka na ploche, vývoj krivky. modelovanie lesných požiarov, topologcké zmeny

Contents

1 Introduction

Nowadays there exist several mathematical fire propagation models and simulation softwares. We can divide them according to the way they simulate the fire propagation proceses to (quasi-) physical, e.g. Wildland Fire Dynamics Simulator, and (quasi-) empirical, e.g. FARSITE. In general, the simulations based on the physical models are more time-consuming, comparing to the empirical models. A number of wildland fire simulation models is builton empirical models, either vector-based (Farsite, Prometheus, SiroFire) or on raster-based approaches (Vesta, Flire, Ignite, Firestation, Pyrocart) [27].

In the mathematical literature, there exists a number of studies about the evolution of planar and surface curves with many various applications, see e.g. [1–7, 9, 11, 12, 16–22, 26]. We distinguish two main approaches to handle the curve evolution problems, the so-called Lagrangian (direct) approach, see e.g. [1, 9, 17] and the so-called Eulerian (level-set) approach, see e.g. [22, 26]. In the Eulerian level-set approach, one used to solve the problem of curve evolution in a 2-D computational domain which is usually discretized by a uniform grid and the number of discrete unknowns is proportional to the number of grid points. The evolving curve is obtained implicitly, as the zero isoline of 2-D + time level set function. In the Lagrangian approach one evolves directly the curve discretization points, so it is spatially 1-D problem and thus computationally much more simple and faster than the level-set method. However, the Lagrangian approaches need the so-called tangential grid point redistribution [3, 11, 12, 16–21] and efficient algorithm for the detection and treatment of topological changes in curves evolution [2, 4–7, 20], which are on the other hand automatically handled by the level set method [22, 26]. When the Lagrangian methods are tangentially stabilized and are able to treat the topological changes fastly, they represent really efficient approach to 2-D or surface curve evolution.

This thesis is organized as follows. We define a surface curve as a fire perimeter in Chapter 2. We design the outer normal velocity and derive the external driving forces for the surface curve evolution in Chapter 3. We also employ the tangential velocity in order to obtain asymptotically uniform grid point redistribution. Numerical discretization is presented in Chapter 4. In the Chapter 5 we discuss the efficient treatment of topological changes in the fire perimeter, splitting and merging of the curves. In the last Chapter 6, the results of our model on representative examples are presented.

2 Surface curve

In this thesis we will use the so-called Lagrangian approach to the evolution of a surface curve, representing a fire perimeter. For numerical computations we will use its projection into a planar curve, where we follow [17, 19].

Let us have a planar curve Γ, $\Gamma : S^1 \to \mathbb{R}^2$, parametrized by $u \in S^1$, where S^1 is a circle with unit length, thus $u \in [0,1]$ and $\Gamma = \left\{\mathbf{x}(u); u \in S^1\right\}$, where $\mathbf{x}(u) = (x(u), y(u))$ is the position vector of the curve Γ for parameter u.

We suppose, that the curve will expand due to an external force. In other words, we suppose the motion of the curve in the outer normal direction. If the curve Γ is parametrized in a counterclockwise direction, the unique definition of the unit tangent $\mathbf{T}$ and outer unit normal $\mathbf{N}$ vectors to the planar curve Γ can be done as follows: $\mathbf{T} = \mathbf{x}_s$, $\mathbf{N} = \mathbf{x}_s^{\perp}$ and $\mathbf{T} \wedge \mathbf{N} = -1$, where $\mathbf{T} \wedge \mathbf{N}$ denotes the determinant of the matrix with columns $\mathbf{T}$ and $\mathbf{N}$, where s is the unit arc-length parametrization of the curve Γ: $ds = g du$, where $g = |\mathbf{x}_u| > 0$. If $\mathbf{T} = (x_s, y_s)$, then $\mathbf{N} = (y_s, -x_s)$.

Such curve could represent the fire perimeter on a horizontal plane [2]. Unfortunately, in the most cases the wildland fires do not occur on the flat terrain. Therefore we define a surface $\mathcal{M}$, that represents a local Earth topography, given e.g. by a digital terrain model. Let $\mathcal{M}$ be the two-dimensional surface in $\mathbb{R}^3$, $\mathcal{M} = \left\{(x, y, \varphi(x,y)) \in \mathbb{R}^3, (x,y) \in \Omega\right\}$, represented by a graph of a function $\varphi : \Omega \subset \mathbb{R}^2 \to \mathbb{R}$ defined in a domain $\Omega \subset \mathbb{R}^2$. Let the curve $\mathcal{G} : S^1 \to \mathbb{R}^3$, parametrized by $u \in S^1$, where S^1 is a circle with unit length, thus $u \in [0,1]$, be a smooth surface curve on $\mathcal{M}$, that represents the fire perimeter on the surface $\mathcal{M}$. Let us denote by p the unit arc-length parametrization of the curve $\mathcal{G}$: $dp = G du$, where $G = |\mathcal{G}_u| > 0$. Furthermore, we suppose a constraint between the planar curve Γ and the surface curve $\mathcal{G}$ as follows $\mathcal{G} = \left\{(x(u), y(u), z(u) = \varphi(x(u), y(u))) \in \mathbb{R}^3, (x(u), y(u)) \in \Gamma\right\}$, so that the curve Γ is a vertical projection of the surface curve $\mathcal{G}$.. Now we can define the formula for the unit tangent $\mathcal{T}$ and unit normal vectors $\mathcal{N}$ in the tangent plane to surface $\mathcal{M}$. For the unit tangent vector $\mathcal{T}$ we obtain subsequently

$$\mathcal{T} = \frac{(\mathbf{T}, \nabla\varphi \cdot \mathbf{T})}{\sqrt{1 + (\nabla\varphi \cdot \mathbf{T})^2}}. \tag{2.1}$$

We find $\mathcal{N}$ as a cross product of the unit tangent vector $\mathcal{T}$ and the upward-pointing unit normal vector to the surface $\mathcal{M}$. Vector $\mathcal{N}_{\mathcal{M}}$ is given as a cross product of two vectors from the tangent plane to the surface $\mathcal{M}$, e.g. $\mathbf{v_1} = (1, 0, \varphi_x)$ and $\mathbf{v_2} = (0, 1, \varphi_y)$, which is then normalized and we get

$$\mathcal{N}_{\mathcal{M}} = \frac{(-\varphi_x, -\varphi_y, 1)}{\sqrt{1 + |\nabla\varphi|^2}} = \frac{(-\nabla\varphi, 1)}{\sqrt{1 + |\nabla\varphi|^2}}. \tag{2.2}$$

Then the outer unit normal vector $\mathcal{N}$ is given as follows

$$\mathcal{N} = \frac{\left(\left(1 + (\nabla\varphi \cdot \mathbf{T})^2\right)\mathbf{N} - (\nabla\varphi \cdot \mathbf{T})(\nabla\varphi \cdot \mathbf{N})\mathbf{T}, \nabla\varphi \cdot \mathbf{N}\right)}{\sqrt{\left(1 + |\nabla\varphi|^2\right)\left(1 + (\nabla\varphi \cdot \mathbf{T})^2\right)}}. \tag{2.3}$$

For the surface curve $\mathcal{G}$ we find its curvature vector $\mathcal{K}$ as the second derivative of $\mathcal{G}$ with respect to p

$$\mathcal{K} = \frac{\left(-k\mathbf{N}\left(1+(\nabla\varphi\cdot\mathbf{T})^2\right) - \mathbf{T}(\nabla\varphi\cdot\mathbf{T})\mathbf{T}^T H(\varphi)\mathbf{T} - k(\nabla\varphi\cdot\mathbf{N}),\ \mathbf{T}^T H(\varphi)\mathbf{T} - k(\nabla\varphi\cdot\mathbf{N})\right)}{\left(1+(\nabla\varphi\cdot\mathbf{T})^2\right)^2}, \quad (2.4)$$

where k is the planar curve curvature and $H(\varphi)$ is the Hessian of the terrain function φ.

From the Darboux frame, which is the analog of the Frenet-Serret frame, we know that $\mathcal{K} = K_g \cdot (-\mathcal{N}) + K_n \cdot \mathcal{N}_{\mathcal{M}}$, where K_g is a geodesic curvature and K_n is a normal curvature. The splitting of the curvature $\mathcal{K}$ to K_g and K_n is important for fire spread simulation. If we know the curvature in the tangent plane, K_g, we know how the fire perimeter shape influences the local normal velocity. The second part, K_n, expresses the variable surface (canyons, valleys, ridges) contribution to the local normal velocity. Since the geodesic curvature is a projection of $\mathcal{K}$ to the inner unit normal vector $-\mathcal{N}$ we get

$$K_g = k\frac{\sqrt{1+|\nabla\varphi|^2}}{\left(1+(\nabla\varphi\cdot\mathbf{T})^2\right)^{\frac{3}{2}}} - \frac{(\nabla\varphi\cdot\mathbf{N})\,\mathbf{T}^T H(\varphi)\mathbf{T}}{\sqrt{1+|\nabla\varphi|^2}\left(1+(\nabla\varphi\cdot\mathbf{T})^2\right)^{\frac{3}{2}}}. \quad (2.5)$$

The normal curvature is the component of $\mathcal{K}$ in the direction of the unit upward-pointing normal vector to the surface $\mathcal{N}_{\mathcal{M}}$

$$K_n = \frac{\mathbf{T}^T H(\varphi)\mathbf{T}}{\left(1+(\nabla\varphi\cdot\mathbf{T})^2\right)\sqrt{1+|\nabla\varphi|^2}}. \quad (2.6)$$

3 Wildland surface fire spread mathematical model

In this Chapter we describe the forces influencing a surface curve evolution. We characterize an outer normal velocity $\mathcal{V}$ of the surface curve $\mathcal{G}$, an external force $\mathcal{F}$ and its influencing factors, such as fuel, wind and terrain slope. We also derive the general form of the planar (projected) curve evolution, where we split the planar velocity into the normal velocity β and the tangential velocity α. While the normal velocity changes the curve shape, the tangential velocity is used for the redistribution of curve points.

3.1 Normal velocity of the surface curve

The normal velocity is expressed by an external force $\mathcal{F}$ and by the shape of the fire perimeter. The geodesic curvature on the tangent plane to a surface, K_g, smooths the curve. Moreover, the shape of a topography influences the normal velocity. The normal curvature K_n of the curve evolving in a valley (or on a ridge) can increase (or decrease) the normal velocity $\mathcal{V}$. Such evolution of the curve $\mathcal{G}$ can be described by following velocity $\mathcal{V}$ in the outer normal direction

$$\mathcal{V} = \mathcal{F}\left(\delta_{\mathcal{F}} - \delta_g \mathcal{K}_g + \delta_n \mathcal{K}_n\right), \tag{3.1}$$

where $\mathcal{F}$ is an external force, δ_g is a weight of the geodesic curvature and δ_n is a weight of the normal curvature influence to the fire spread. Such formula expresses the dominant role of an external force, that can be accelerated or slowed down by the geodesic and normal curvatures. A design of an external force influencing the fire behavior is based on the empirical laws of the wildland fire perimeter propagation. Research indicates, that wildland fire propagation is influenced by fuel parameters, weather conditions and surrounding topography slope. We suggest following formula for the external force

$$\mathcal{F} = f\, f_w(\mathbf{w}\cdot\mathcal{N})\, f_s(\mathbf{s}\cdot\mathcal{N}), \tag{3.2}$$

where f is a fuel influence, $f_w(\mathbf{w}\cdot\mathcal{N})$ is a wind influence and $f_s(\mathbf{s}\cdot\mathcal{N})$ is a terrain slope influence on the rate of spread, with $\mathbf{w}$ being a three dimensional wind vector, $\mathbf{s}$ being a three dimensional slope vector and $\mathcal{N}$ being the unit normal vector to the surface .

Fuel influence. In our model we shall consider a surface fuel. We assume heterogeneous fuel flammability on a topographic surface. Therefore, the ROS map is a scalar function $f(\mathbf{x})$ given on a topography. According to the literature [13], we suppose, that the ROS map is given by weighted combination of the most important factors, such as species, age, bulk density, fuel moisture, fuel loading and compactness. Some of these factors can be determined by a typological forestry maps, like the species, age or bulk density, and their combination creates the ROS map.

Wind influence. Wind can dramatically increase (or decrease) the fire spread rate if the fire spreads in (or against) the wind direction. Wind increases the fuel preheating, drying and it supplies the oxygen to the fire. We consider that wind has the same speed and direction on the whole topography given by a two-dimensional vector $\mathbf{w}^{2D}$. While we retain the length, we construct the third coordinate as the directional derivative of the terrain function φ along a vector $\mathbf{w}^{2D}$, i. e. $\mathbf{w} = \left(\mathbf{w}^{2D}, \nabla\varphi\cdot\mathbf{w}^{2D}\right)\frac{\left|\mathbf{w}^{2D}\right|}{\sqrt{\left|\mathbf{w^{2D}}\right|^2+\left(\nabla\varphi\cdot\mathbf{w}^{2D}\right)^2}}$. According [25, 28] the wind influences the rate of spread exponentially, so we consider the scalar product of the wind vector $\mathbf{w}$ and the outer normal vector $\mathcal{N}$ as an exponent of a function f_w in the form $f_w(\mathbf{w}\cdot\mathcal{N}) = e^{\lambda_w(\mathbf{w}\cdot\mathcal{N})}$, where λ_w is a positive parameter.

Topography slope influence. A slope, similarly to wind, can increase (or decrease) the fire spread or change the spread direction. Slope increases the radiation and convection heat transfer up the slope. From the digital terrain model (the topography function φ) we can easily obtain the vector function $\nabla\varphi$ characterizing a topography slope. Now, we compute the third coordinate of a slope vector $\mathbf{s}$ in the tangent plane to the surface $\mathcal{M}$, while we retain its length. We obtain the third coordinate of a vector $\mathbf{s}$ as the directional derivative of the terrain function φ along $\nabla\varphi$, i.e. $\mathbf{s} = \left(\nabla\varphi, |\nabla\varphi|^2\right) \frac{|\nabla\varphi|}{\sqrt{|\nabla\varphi|^2 + \left(|\nabla\varphi|^2\right)^2}} = \frac{\left(\nabla\varphi, |\nabla\varphi|^2\right)}{\sqrt{1+|\nabla\varphi|^2}}$. According to [8, 28], slope influences the rate of spread exponentially, depending on the projection of $\mathbf{s}$ to $\mathcal{N}$, therefore we consider $f_s(\mathbf{s}\cdot\mathcal{N}) = e^{\lambda_s(\mathbf{s}\cdot\mathcal{N})}$, where λ_s is a positive parameter.

3.2 Evolution of the projected planar curve

We suppose that the projected planar curve Γ of the surface curve $\mathcal{G}$, which models the fire spread, move in time by a general planar velocity vector field v. We can split such general motion of any point $\mathbf{x}$ of the curve Γ into the normal and tangential directions, so we consider a general form of the planar curve evolution in the following form

$$\mathbf{x}_t = v = \beta\mathbf{N} + \alpha\mathbf{T}, \tag{3.3}$$

where β is a velocity in the normal direction $\mathbf{N}$ and α is a tangential velocity of the planar curve Γ. In Section 3.1 we designed the normal velocity $\mathcal{V}$ for the surface curve $\mathcal{G}$. Now we want to relate the normal velocity $\mathcal{V}$ in the tangent plane to the projected curve Γ normal velocity β. Following [17] we get subsequently, that

$$\mathcal{V} = \mathcal{G}_t \cdot \mathcal{N} = (x_t, y_t, \varphi_t(x,y)) \cdot \mathcal{N} = (\mathbf{x}_t, \mathbf{x}_t \cdot \nabla\varphi) \cdot \mathcal{N} = \sqrt{\frac{1+|\nabla\varphi|^2}{1+(\nabla\varphi\cdot\mathbf{T})^2}}\beta, \tag{3.4}$$

from where we obtain

$$\beta = \mathcal{V}\sqrt{\frac{1+(\nabla\varphi\cdot\mathbf{T})^2}{1+|\nabla\varphi|^2}}. \tag{3.5}$$

Employing the equation for the normal velocity of surface curve (3.1), geodesic (2.5) and normal curvatures (2.6), taking into account the Frenet equation $\mathbf{x}_{ss} = -k\mathbf{N}$ the equation for the normal velocity of the planar curve (3.5) can be written in the form $\beta = (-\varepsilon k + w)$. Now, we rewrite (3.3) to the form of the intrinsic PDE for the evolution of the position vector $\mathbf{x}$ of the planar curve Γ

$$\mathbf{x}_t = \varepsilon\mathbf{x}_{ss} + \alpha\mathbf{x}_s + w\mathbf{x}_s^{\perp}, \tag{3.6}$$

where

$$\varepsilon = \frac{\mathcal{F}\delta_g}{1+(\nabla\varphi\cdot\mathbf{T})^2}, \tag{3.7}$$

$$w = \mathcal{F}\left(\delta_{\mathcal{F}}\sqrt{\frac{1+\left(\nabla\varphi\cdot\mathbf{T}\right)^2}{1+|\nabla\varphi|^2}} + \delta_g \frac{\mathbf{T}^T H(\varphi)\mathbf{T}(\nabla\varphi\cdot\mathbf{N})}{\left(1+(\nabla\varphi\cdot\mathbf{T})^2\right)\left(1+|\nabla\varphi|^2\right)} + \delta_n \frac{\mathbf{T}^T H(\varphi)\mathbf{T}}{\sqrt{1+(\nabla\varphi\cdot\mathbf{T})^2}\left(1+|\nabla\varphi|^2\right)}\right) \tag{3.8}$$

and a suitable choice of α is discussed in the following Section.

3.3 The choice of the tangential velocity

Although it is well-known that a tangential motion does not change the shape of an evolving curve, it is helpful in stabilization of the numerical algorithms based on Lagrangian approaches [16, 18] in a number of applications [1, 2, 16–21].

In this application, we use the redistrbution for planar curve [2, 18]. Since we represent fire perimeter with the surface curve we design the tangential velocity for asymptotically uniform redistribution of surface curve points similarly to the redistributions already mentioned above in the form

$$\psi_p = K_g\mathcal{V} - \langle K_g\mathcal{V}\rangle_{\mathcal{G}} + \omega\left(\frac{\mathcal{L}}{G} - 1\right), \tag{3.9}$$

where ψ is a tangential velocity of a surface curve, $\langle K_g\mathcal{V}\rangle_{\mathcal{G}} = \frac{1}{\mathcal{L}}\int_{\mathcal{G}} K_g\mathcal{V}dp$, ω is a parameter determining how fast the redistribution becomes uniform and $\mathcal{L}$ is a surface curve length.

Since we evolve the planar curve, we need to find tangential velocity α for planar curve. Similarly to formula (3.5) between planar β and surface $\mathcal{V}$ normal velocity, we obtain relation between tangential velocities in the plane and in the surface. Considering (3.3) we get

$$\psi = \mathbf{X}_t\cdot\mathcal{T} = (x_t, y_t, \varphi_t(x,y))\cdot\mathcal{T} = (\mathbf{x}_t, \mathbf{x}_t\cdot\nabla\varphi)\cdot\mathcal{T} = \alpha\sqrt{1+(\nabla\varphi\cdot\mathbf{T})^2} + \beta\frac{(\nabla\varphi\cdot\mathbf{N})(\nabla\varphi\cdot\mathbf{T})}{\sqrt{1+(\nabla\varphi\cdot\mathbf{T})^2}}, \tag{3.10}$$

from where we obtain

$$\alpha = \frac{\psi}{\sqrt{1+(\nabla\varphi\cdot\mathbf{T})^2}} - \beta\frac{(\nabla\varphi\cdot\mathbf{N})(\nabla\varphi\cdot\mathbf{T})}{\sqrt{1+(\nabla\varphi\cdot\mathbf{T})^2}}. \tag{3.11}$$

4 Numerical scheme

In the previous Chapter, we derived the intrinsic PDE for the planar curve Γ position vector $\mathbf{x}$ evolution

$$\mathbf{x}_t - \alpha\mathbf{x}_s = \varepsilon\mathbf{x}_{ss} + w\mathbf{x}_s^{\perp} \tag{4.1}$$

and here we present its numerical discretization. The discretization is based on the flowing finite volume method in space [16] and the semi-implicit discretization [2, 16] in time. To guarantee the solvability of arising cyclic tridiagonal linear systems for any choice of time step, we use the so-called inflow-implicit/outflow-explicit (IIOE) scheme [2, 14, 15] in approximation of advection term.

In order to perform the time discretization, let us denote by m the time step numbering and by τ the length of discrete time step. Let us approximate the time derivative by the finite difference $(\mathbf{x}_i)_t = \frac{\mathbf{x}_i^{m+1}-\mathbf{x}_i^m}{\tau}$. Taking the inflow part of advection term and the curvature term implicitly and the outflow part of the advection term and the force term explicitly, we obtain the fully discrete scheme in form of cyclic tridiagonal system

$$\mathbf{x}_{i-1}^{m+1}\left(-\frac{\varepsilon_i^m}{h_i^m}-\frac{b_{i-\frac{1}{2}}^{in}}{2}\right)+\mathbf{x}_{i+1}^{m+1}\left(-\frac{\varepsilon_i^m}{h_{i+1}^m}-\frac{b_{i+\frac{1}{2}}^{in}}{2}\right)+\mathbf{x}_i^{m+1}\left(\frac{h_{i+1}^m+h_i^m}{2\tau}+\frac{\varepsilon_i^m}{h_i^m}+\frac{\varepsilon_i^m}{h_{i+1}^m}+\frac{b_{i-\frac{1}{2}}^{in}}{2}+\frac{b_{i+\frac{1}{2}}^{in}}{2}\right)=$$

$$=\mathbf{x}_i^m\frac{h_{i+1}^m+h_i^m}{2\tau}-\frac{b_{i+\frac{1}{2}}^{out}}{2}\left(\mathbf{x}_i^m-\mathbf{x}_{i+1}^m\right)-\frac{b_{i-\frac{1}{2}}^{out}}{2}\left(\mathbf{x}_i^m-\mathbf{x}_{i-1}^m\right)+w_i^m\left(\frac{\mathbf{x}_{i+1}^m-\mathbf{x}_{i-1}^m}{2}\right)^{\perp}, \quad (4.2)$$

$i=1,\ldots,n$, where n is a number of curve grid points.

In the complex fire simulations, e.g. when curves are merging or splitting, the evolving fire perimeter can be locally sharp, even with singularities. In such singular points we use just the first order implicit upwind instead of the second order IIOE method in the advection term. This upwind scheme is applied when the angle between two consecutive curve segments $(\mathbf{x}_{i-1},\mathbf{x}_i)$ and $(\mathbf{x}_i,\mathbf{x}_{i-1})$ is less than $120°$. In the upwind scheme we use only inflow velocities $b_{i-\frac{1}{2}}^{in}$, $b_{i+\frac{1}{2}}^{in}$, and points $\mathbf{x}_{i-\frac{1}{2}}$, $\mathbf{x}_{i+\frac{1}{2}}$ are approximated by the neighbouring values $\mathbf{x}_{i-1}$ or $\mathbf{x}_{i+1}$, depending on inflow direction. In such way we get

$$\mathbf{x}_{i-1}^{m+1}\left(-\frac{\varepsilon_i^m}{h_i^m}-b_{i-\frac{1}{2}}^{in}\right)+\mathbf{x}_{i+1}^{m+1}\left(-\frac{\varepsilon_i^m}{h_{i+1}^m}-b_{i+\frac{1}{2}}^{in}\right)$$

$$+\mathbf{x}_i^{m+1}\left(\frac{h_{i+1}^m+h_i^m}{2\tau}+\frac{\varepsilon_i^m}{h_i^m}+\frac{\varepsilon_i^m}{h_{i+1}^m}+b_{i-\frac{1}{2}}^{in}+b_{i+\frac{1}{2}}^{in}\right)=\mathbf{x}_i^m\frac{h_{i+1}^m+h_i^m}{2\tau}+w_i^m\left(\frac{\mathbf{x}_{i+1}^m-\mathbf{x}_{i-1}^m}{2}\right)^{\perp} \quad (4.3)$$

instead of (4.2). This replacement of (4.2) by (4.3) occurs rarely, but in case it arises, the usage of (4.3) makes the scheme robust with respect to singularities.

The above system is strictly diagonally dominant, thus it is always solvable by the efficient cyclic tridiagonal solver without any restriction on time step length τ [2].

In the numerical schemes (4.2) and (4.3) there are parameters ε_i^m and w_i^m, given by (3.7)-(3.8), which are evaluated as follows

$$\varepsilon_i^m=\frac{\mathcal{F}_i^m\delta_g}{1+(\nabla\varphi_i^m.\mathbf{T}_i^m)^2},$$

$$w_i^m=\mathcal{F}_i^m\left(\delta_{\mathcal{F}}\sqrt{\frac{1+\left(\nabla\varphi_i^m.\mathbf{T}_i^m\right)^2}{1+\left|\nabla\varphi_i^m\right|^2}}+\delta_g\frac{\mathbf{T}_i^{mT}H\left(\varphi_i^m\right)\mathbf{T}_i^m\nabla\varphi_i^m.\mathbf{N}_i^m}{\left(1+\left(\nabla\varphi_i^m.\mathbf{T}_i^m\right)^2\right)\left(1+\left|\nabla\varphi_i^m\right|^2\right)}+\delta_n\frac{\mathbf{T}_i^{mT}H\left(\varphi_i^m\right)\mathbf{T}_i^m}{\sqrt{1+\left(\nabla\varphi_i^m.\mathbf{T}_i^m\right)^2}\left(1+\left|\nabla\varphi_i^m\right|^2\right)}\right),$$

where $\varphi_i^m=\varphi\left(\mathbf{x}_i^m\right)$, $\mathbf{T}_i^m=\frac{\mathbf{x}_{i+1}^m-\mathbf{x}_{i-1}^m}{h_{i+1}^m+h_i^m}$, $\mathbf{N}_i^m=\mathbf{T}_i^{m\perp}$ and $\mathcal{F}_i^m$, $\nabla\varphi_i^m$ and $H\left(\varphi_i^m\right)$ are discrete values of the external force, topography slope and the square matrix of second-order partial derivatives of the topography function φ, which we obtain by a bilinear interpolation.

In order to discretize the tangential velocity α_i first we set $\alpha_0^m=0$, which would cause that the point $\mathbf{x}_0$ will move only along its normal direction. Then we get α_i^m for

$i = 1, 2, ..., n-1$ by

$$\alpha_i^m = \alpha_{i-1}^m + h_i^m k_i^m \beta_i^m - h_i^m \langle k\beta \rangle_\Gamma^m + \omega \left(\frac{L^m}{n} - h_i^m \right), \tag{4.4}$$

where

$$k_i^m = \operatorname{sgn}\left(\mathbf{h}_{i-1}^m \wedge \mathbf{h}_{i+1}^m\right) \frac{1}{2h_i^m} \arccos\left(\frac{\mathbf{h}_{i+1}^m \cdot \mathbf{h}_{i-1}^m}{h_{i+1}^m h_{i-1}^m} \right), \tag{4.5}$$

$$\beta_i^m = -\frac{\varepsilon_{i-1}^m + \varepsilon_i^m}{2} k_i^m + \frac{w_{i-1}^m + w_i^m}{2}, \tag{4.6}$$

$$\langle k\beta \rangle_\Gamma = \frac{1}{L^m} \sum_{l=1}^{n} h_l^m k_l^m \beta_l^m, \tag{4.7}$$

$$L^m = \sum_{l=1}^{n} h_l^m, \tag{4.8}$$

where $\mathbf{h}_i^m = \mathbf{x}_i^m - \mathbf{x}_{i-1}^m$, $h_i^m = |\mathbf{h}_i^m|$.

In case of the point redistribution on a surface we get α_i^m by the following formula

$$\alpha_i^m = \frac{\psi_i^m}{\sqrt{1 + (\nabla\varphi_i^m \cdot \mathbf{T}_i^m)^2}} - \beta_i^m \frac{(\nabla\varphi_i^m \cdot \mathbf{N}_i^m)(\nabla\varphi_i^m \cdot \mathbf{T}_i^m)}{\sqrt{1 + (\nabla\varphi_i^m \cdot \mathbf{T}_i^m)^2}} \tag{4.9}$$

and ψ_i^m are obtained similarly to α_i^m discretization. We set $\psi_0^m = 0$ and ψ_i^m for $i = 1, 2, ..., n-1$ by

$$\psi_i^m = \psi_{i-1}^m + \mathcal{H}_i^m {K_g}_i^m \mathcal{V}_i^m - \mathcal{H}_i^m \left\langle K_g \mathcal{V} \right\rangle_{\mathcal{G}}^m + \omega \left(\frac{\mathcal{L}^m}{n} - \mathcal{H}_i^m \right), \tag{4.10}$$

where

$$\mathcal{H}_i^m = \left| (\mathbf{x}_i^m, \varphi_i^m) - \left(\mathbf{x}_{i-1}^m, \varphi_{i-1}^m\right) \right|, \tag{4.11}$$

$${K_g}_i^m = k_i^m \frac{\sqrt{1 + \left|\nabla\varphi_i^m\right|^2}}{\left(1 + (\nabla\varphi_i^m \cdot \mathbf{T}_i^m)^2\right)^{\frac{3}{2}}} - \frac{(\nabla\varphi_i^m \cdot \mathbf{N}_i^m)\, \mathbf{T}_i^{mT} H(\varphi_i^m)\, \mathbf{T}_i^m}{\sqrt{1 + \left|\nabla\varphi_i^m\right|^2} \left(1 + (\nabla\varphi_i^m \cdot \mathbf{T}_i^m)^2\right)^{\frac{3}{2}}}, \tag{4.12}$$

$$\mathcal{V}_i^m = \sqrt{\frac{1 + \left|\nabla\varphi_i^m\right|^2}{1 + (\nabla\varphi_i^m \cdot \mathbf{T}_i^m)^2}} \beta_i^m, \tag{4.13}$$

$$\mathcal{L}^m = \sum_{l=1}^{n} \mathcal{H}_l^m, \tag{4.14}$$

$$\left\langle K_g \mathcal{V} \right\rangle_{\mathcal{G}}^m = \frac{1}{\mathcal{L}^m} \sum_{l=1}^{n} \mathcal{H}_l^m K_{g\,l}^{\,m} \mathcal{V}_l^m. \tag{4.15}$$

Setting $\alpha_0^m = 0$ can cause an unnecessary tangential motion in effort to redistribute the curve points uniformly. To minimize the tangential velocity, we find the average tangential velocity $\alpha_{avg}^m = \sum\limits_{i=0}^{n} \frac{\alpha_i^m}{n}$. It is clear, that α_{avg}^m is the unnecessary tangential velocity and therefore we find new minimized values as $\overline{\alpha_i^m} = \alpha_i^m - \alpha_{avg}^m$ for $i = 0, 1, \ldots, n$, by which we redefine α_i^m.

5 Topological changes treatment

By a topological change we mean a merging of several fire perimeters and/or a splitting of the evolving curve into several separate curves. Such splitting can occur when the curve velocity is locally slowed down significantly (e.g. nonburnable regions). Detecting and solving the topological changes in the Lagrangian approach is usually highly time consuming [10], because the standard approaches have computational complexity $O\left(n^2\right)$, where n is the number of curve points. Such complexity is due to a strategy for the topological changes detection, which consists of computing pairwise distances between all grid points of the curve [10, 23] and slows down the overall computing time significantly. We present our $O(n)$ approach for the detection and processing of the topological changes in the curves evolution which makes our overall computational method fast and applicable in a complex situation of a fire perimeter evolution. In the sequel we omit the time step index m, since we detect the topological changes before every time step. Our overall computing strategy can be described by the Algorithm 1, where $\overline{h}_j$ is mean segment length of curve Γ_j and h_d is a desired segment length.

Algorithm 1: Overall computing strategy

---

foreach *Time step* **do**
  Topological changes detection (splitting)
  Topological changes detection (merging)
  foreach *Curve* Γ_j **do**
    if $\left|h_d - \overline{h}_j\right| > \varepsilon_h$ **then**
      Adding and removing grid points
    Numerical computation by the scheme (4.2), (4.3)

In our method every curve is asymptotically uniformly discretized, i.e. all segment lengths of curve are close to their mean value $\overline{h}_j$. However, $\overline{h}_j$ can differ for different curves, it may increase for expanding curves or decrease for shrinking curves. Such difference in $\overline{h}_j$ is non-desirable, especially in merging of curves, so we maintain the desired segment length h_d for all curves by adding or removing points in the longest or shortest segments to get the appropriate number of points. Then the asymptotically uniform redistribution is quickly obtained by the tangential velocity included in the numerical method.

Our main idea for the topological changes detection, see also [2], is to create a narrow strip of cells along the curves. Let us have an array $p[I][J]$, where $I = 0, ..., py$, $J = 0, ..., px$, covering the whole computational domain Ω. It is crucial to set the coupling between the cell size and the desired curve segment length h_d, especially when treating the curve splitting. To that goal we set the cell size to $2h_d \times 2h_d$, which ensures maximally three points (two whole segments) of the smooth curve in one cell, because the cell diagonal length is less than $3h_d$. In our approach we will split the curve if two non-neighboring curve grid points belong to the same cell. We also require that the difference of indexes of such two non-neighboring grid points should be larger than or equal to three. This means that the curve should leave the cell and come back to the cell following the curve trajectory between those two points, because four consecutive points cannot belong to one cell. In such case we split the curve. Merging detection is very similar, since we detect whether two points of different curves belongs to the same cell. If so, we merge those curves.

Splitting the curve Γ_j at points $\mathbf{x}_{j,s_1}$ and $\mathbf{x}_{j,s_2}$ into two closed curves is done as follows. The first point set $\mathbf{x}_{j,1}$, $\mathbf{x}_{j,2}$, ..., $\mathbf{x}_{j,s_1-1}$, $\mathbf{x}_{j,s_2+1}$, ..., $\mathbf{x}_{j,n}$ will replace the original curve with number j. The second point set $\mathbf{x}_{j,s_1+1}$, $\mathbf{x}_{j,s_1+2}$, ..., $\mathbf{x}_{j,s_2-2}$, $\mathbf{x}_{j,s_2-1}$ will be stored as Γ_{NC+1}. Merging curves Γ_{c_1} and Γ_{c_2} at points $\mathbf{x}_{c_1,m_1}$ and $\mathbf{x}_{c_2,m_2}$ is treated similarly. The newly merged curve will consist of $n_{c_1} + n_{c_2} - 2$ points, namely $\mathbf{x}_{c_1,1}$, ..., $\mathbf{x}_{c_1,m_1-1}$, $\mathbf{x}_{c_2,m_2+1}$, $\mathbf{x}_{c_2,n_{c_2}}$, $\mathbf{x}_{c_2,1}$, ..., $\mathbf{x}_{c_2,m_2-1}$, $\mathbf{x}_{c_1,m_1+1}$, $\mathbf{x}_{c_1,n_{c_1}}$, and will be stored as curve Γ_{c_1}. The curve Γ_{c_2} will be deleted.

We note, that due to the topological changes detection we use time step $\tau \le 2h_d/\beta$ which prevents the grid points from skipping through the cell in one time step.

6 Numerical experiments

In this Chapter we describe various numerical experiments showing the properties of our mathematical model. We show, how the curve evolution is influenced by the external force (ROS, wind speed and direction and topography slope), the geodesic and normal curvatures on an artificial topography. We present a reconstruction of the simulated surface fire and we optimize the model parameters.

Comparison of the curve point redistributions In this experiment, we compare the tangential redistributions from Section 3.3. We compare those redistributions on a simple case, where the topography is given by a graph of a function $\varphi(x,y) = 0.1x^2 + y$, 10^4 time steps with time step length 10^{-3} and 100 curve grid points. We set $\omega = 100$, $f = 1, \delta_{\mathcal{F}} = 1$, $\delta_g = 1$, $\delta_n = 1$, $\lambda_s = 1$ and $\lambda_w = 0$. The results at the final time step are very similar visually as well as the Mean Hausdorff distance is very low ($\approx 7 \times 10^{-3}$).

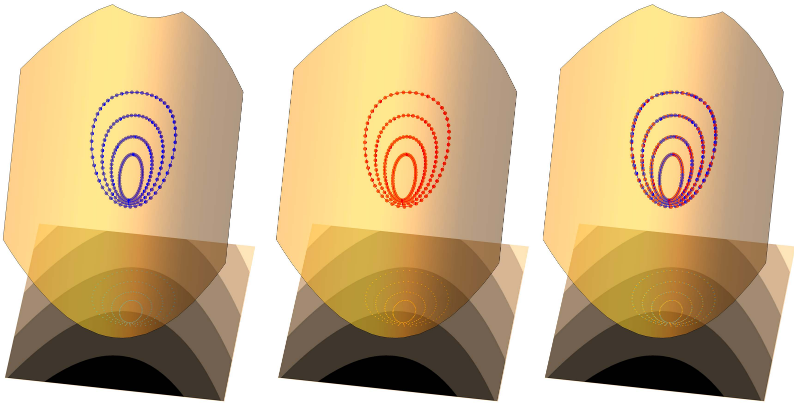

Figure 1: Assymptotically uniform redistribution of the planar curve points (left), surface curve points (center) and their overlay.

The computation with planar curve redistribution is slightly faster, it took $5.31s$. Compared to $5.79s$ for surface curve redistribution it is faster by $0.48s$, which is 9% of the overall computational time. The redistribution of planar curve gives visually unattractive results in variable terrain. On the other hand, the overall computational time is lower, since the computation is more straightforward. Moreover, we need to keep the segment lengths in the planar curve near the desired value. Then, the curve with surface curve redistribution has more points, which leads to longer computations. Although the asymptotically uniform redistribution of the surface curve points seems to be more natural, we use it only for visualization purposes in all further experiments.

Influence of model parameters for evolution on an artificial topography These examples illustrate, how the external force (ROS, wind and terrain slope) influence the curve expanding on a surface. The surface is given by $\varphi(x,y) = 0.1x^2 + y$. We obtain the initial discrete curve as $\mathbf{x}_i^0 = (4\,cos(\gamma_i), 5\,sin(\gamma_i))$, where $\gamma_i = \frac{i}{2\pi}$, $i = 1, \ldots, n$. The number of grid points was set to $n = 100$, the time step was chosen $\tau = \frac{10}{n^2} = 10^{-3}\ min$, number of time steps $NTS = 10000$ and for the tangential velocity we set $\omega = 15$. In the examples we set $f = 1, \delta_{\mathcal{F}} = 1$ and we vary δ_g, δ_n, λ_s and λ_w.

In the experiment presented in Figure 2a we set $f = \delta_{\mathcal{F}} = \lambda_s = \delta_g = \delta_n = 1$, $\lambda_w = 0$, i.e. we consider the fuel influence, terrain slope and the geodesic and normal curvatures. On the other hand, if we employ wind at speed $1\ m.min^{-1}$, $\lambda_w = 1$, we see that the fire spread can be changed significantly. The fire spread can change the direction, e.g. in the case of wind blowing down the valley (Figure 2b) or perpendicular to the valley (Figure 2c) or it can accelerate, if wind blows up the valley (Figure 2d).

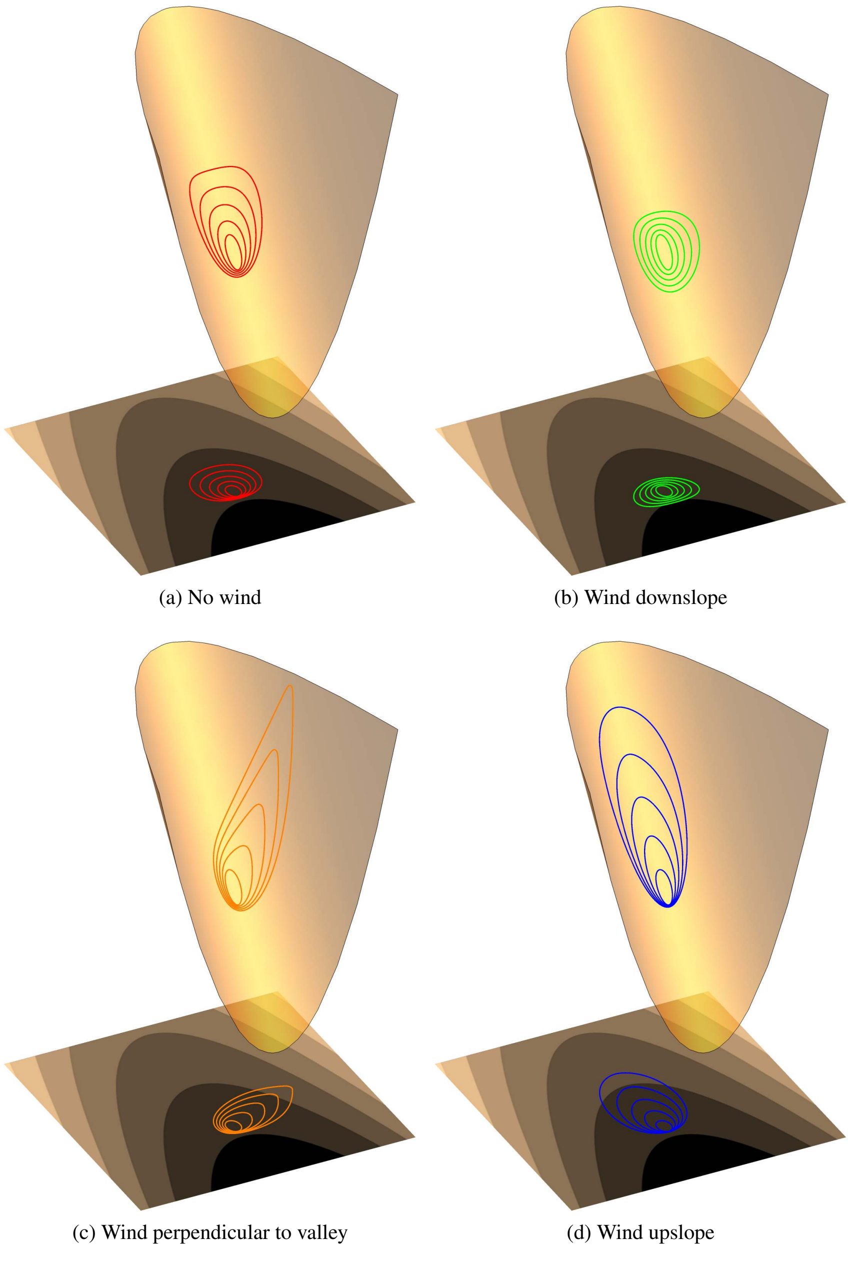

(a) No wind
(b) Wind downslope
(c) Wind perpendicular to valley
(d) Wind upslope

Figure 2: Curve evolution considering fuel, slope influence, geodesic and normal curvature and various wind directions at constant wind speed 1 $m.min^{-1}$.

Real fire reconstruction and model parameters optimization In this experiment, we present the reconstruction of the real grassland fire. Although the fire is small (max. fire perimeter is 79.39 m), it is suitable for finding the model parameters λ_w, λ_s and δ_g. Since the terrain is nearly an inclined plane we do not consider the influence of the normal curvature, $\delta_n = 0$.

The inputs to our model were as follows:

- the initial condition given by segmented fire perimeter 55 s after the ignition,
- homogeneous rate of spread $1.18\, m.min^{-1}$ (measured at place),
- wind velocity and direction (North = 0 deg, East = 90 deg) (measured at place),
- terrain slope given by the digital terrain model.

The video of a fire propagation from a quadcopter was processed using a photogrammetry software to obtain a vertical projection of the fire spread on real terrain to the horizontal plane in $5\,s$ time interval. Then the fire perimeters were segmented manually with the uniform segment length $0.15\,m$ in a CAD software. The desired curve segment length was kept by $h_d = 0.15\ m$, which corresponds to the manual segmentation spatial step and the time step was chosen as $\tau = \frac{h_d^2}{22.5} = 10^{-3}\ min$, i.e. it is proportional to h_d^2.

The Mean Hausdorff distance (MHD) is used as a criterion in inverse modelling, i.e. we use segmented fire perimeters to infer the model parameters. We assume following ranges for the model parameters $\lambda_w \in \langle 0.005, 0.03 \rangle$ with step 0.001, $\lambda_s \in \langle 0.1, 0.5 \rangle$ with step 0.05, $\delta_g \in \langle 0.5, 2.0 \rangle$ with step 0.05. Although the wind direction was measured at place as constantly north (0 deg), the quadcopter video shows variable wind direction. Thus we infer also the wind direction with 0.5 deg step.

We iteratively estimate the parameters values as a constants. From the first iteration of inverse modelling we get average $\overline{\mathrm{MHD}} = 0.289\, m$ and we take the average value $\overline{\lambda_s} = 0.26$ as a constant and estimating the other parameters again. In second iteration, the average $\overline{\mathrm{MHD}} = 0.285\ m$ and we take the average value $\overline{\delta_g} = 0.26$ as a constant too. In the last iteration of inverse modelling we get $\overline{\mathrm{MHD}} = 0.281\ m$ and the average value $\overline{\lambda_w} = 0.26$ is taken as a constant, while we adjust the wind speeds to get the same results with variable λ_w.

We measure accuracy of our fire propagation reconstruction by computing the ratio MHD/L every 5 seconds, where L is the perimeter of the segmented curve. This measure is in range 0.2 - 0.7% in every time moment. We assume that the slight differences between segmented and numerically computed curves, see Fig. 3, could be caused by the fuel heterogeneity (e.g. variable moisture, which is not included in our model, yet) and more dynamic changes in wind direction than the measured and computed in 5 s intervals. The fuel heterogeneity can be seen e.g. in interval 130 - 135 s, see Fig. 3 (i), where the segmented fire perimeter is locally spreading faster. More dynamic changes in wind direction are obvious e.g. in interval 80 - 85 s, see Fig. 3 (d), where the segmented fire perimeter is wider than the computed one. Also the segmentation error is non negligible due to low visibility of fire perimeter through the smoke, see Fig. 3 (h), (i).

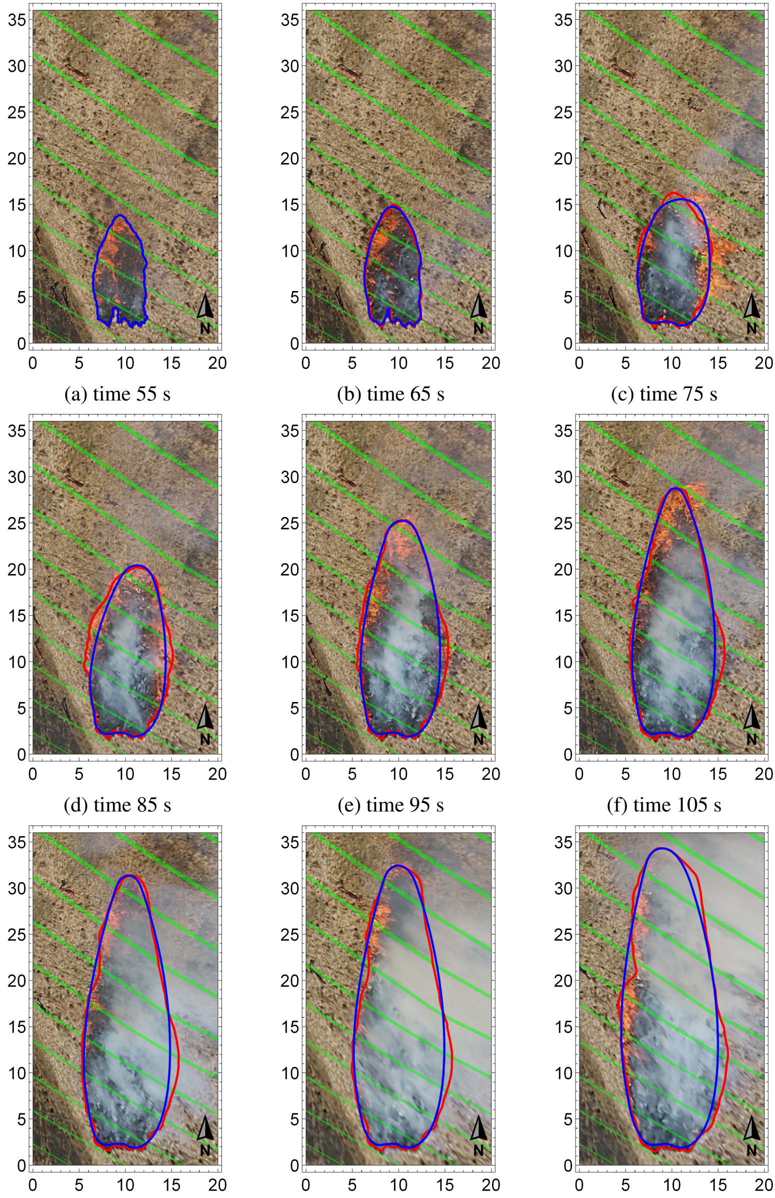

(a) time 55 s (b) time 65 s (c) time 75 s

(d) time 85 s (e) time 95 s (f) time 105 s

(g) time 115 s (h) time 125 s (i) time 135 s

Figure 3: Real fire reconstruction. We compare the manually segmented curve (red) and the curve computed numerically (blue). The initial contition is given by the segmented curve in time 55 s. Contour lines of the digital terrain model (green) are thicker with increasing elevation.

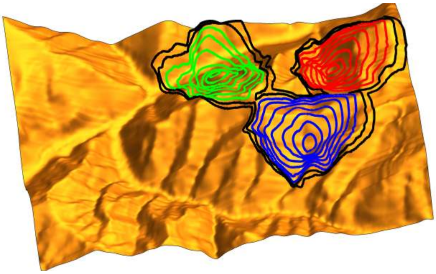

(a) No wind considered

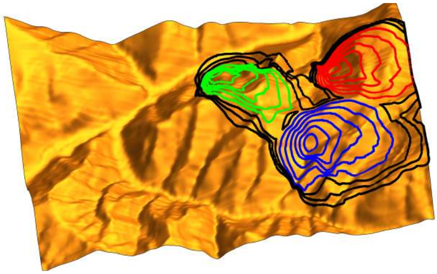

(b) Southeast wind direction (135°)

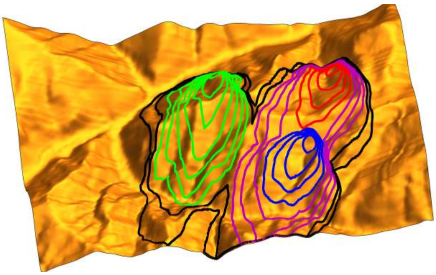

(c) South-Southwest wind direction (202.5°)

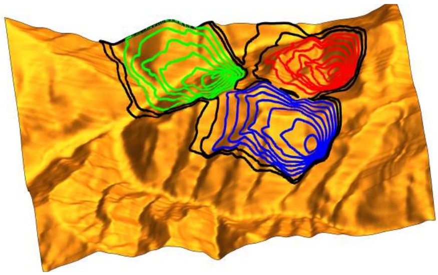

(d) West-Northwest wind direction (292.5°)

Figure 4: Large scale simulation in the area of Staré hory in the central Slovakia, considering homogenous fuel, wind speed $8\,m.min^{-1}$ and various wind directions. The initial condition is given by 3 circles in the vertical projection. Their merging is signalized by the color change (e.g. viloet is merged blue and red curve).

Simulation on a real topography with topological changes We demonstrate the flexibility of our surface fire spread model on the real variable topography of Staré hory in the central Slovakia. The area of 11 km^2 is given by the digital terrain model in 10 m resolution. The wind velocity is set to 8 $m.min^{-1}$. These simulations, considering the model parameters in the range of estimated values from the inverse modelling in the previous experiment, have parameters set as follows $\delta_{\mathcal{F}} = 1$, $\lambda_s = 0.25$, $\lambda_w = 0.02$, $\delta_g = 1$, $\delta_n = 1$, $\omega = 20$, $h_d = 2\,m$ and $\tau = 0.05\,min$. We present the simulations with homogeneous ROS, $f = 1$, and different wind direction, see Fig. 4.

The simulation of 8 hour fire spread took 42.96 s of the computational time for 9600 time steps with 2921.28 curve points per time step at an average.

7 Conclusions

We introduced a new fast and stable forest fire propagation model based on the Lagrangian approach. We described the surface curve, representing the fire perimeter and its projection into the planar curve. Next, we prescribed the mathematical model for the fire perimeter spread over heterogeneous fuel on variable terrain, influenced by wind direction and velocity. Moreover, we considered the influence of the surface fire perimeter shape itself through the geodesic and normal curvatures. The discrete formulation of our model was based on the semi-implicit approach for the curvature term, and the inflow-implicit/outflow-explicit and upwind scheme approaches for the advection term, which allowed any reasonable computational time step choice. We used the tangential velocity to redistribute the grid points along the curve asymptotically uniformly. In addition, we maintained the desired segment length thanks to our strategy for adding and removing points and used tangential velocity. This is useful for our $O(n)$ approach for topological changes treatment of splitting and merging curves. The grassland fire experiment was used to estimate the model parameters. The numerical results revealed the ability of our model to reconstruct the real fire perimeter with minimal error ($< 1\%$).

References

[1] BALAŽOVJECH, M. – MIKULA, K.: *A higher order scheme for a tangentially stabilized plane curve shortening flow with a driving force*: SIAM Journal on Scientific Computing: 33 (2011): pp. 2277–2294.

[2] BALAŽOVJECH, M. – MIKULA, K. – PETRÁŠOVÁ, M. – URBÁN, J.: *Lagrangean method with topological changes for numerical modelling of forest fire propagation*: In: Proceedings of ALGORITMY: 2012: pp. 42–52.

[3] BARRETT, J. W. – GARCKE, H. – NÜRNBERG, R.: *Numerical approximation of gradient flows for closed curves in $\mathbb{R}^d$*: IMA journal of numerical analysis: 30 (2009): pp. 4–60.

[4] BENNINGHOFF, H. – GARCKE, H.: *Efficient image segmentation and restoration using parametric curve evolution with junctions and topology changes*: SIAM Journal on Imaging Sciences: 7 (2014): pp. 1451–1483.

[5] BENNINGHOFF, H. – GARCKE, H.: *Image segmentation using parametric contours with free endpoints*: IEEE Transactions on Image Processing: 25 (2016): pp. 1639–1648.

[6] BENNINGHOFF, H. – GARCKE, H.: *Segmentation and restoration of images on surfaces by parametric active contours with topology changes*: Journal of Mathematical Imaging and Vision: 55 (2016): pp. 105–124.

[7] BENNINGHOFF, H. – GARCKE, H.: *Segmentation of three-dimensional images with parametric active surfaces and topology changes*: J. of Scientific Computing: (2017): pp. 1–35.

[8] BUTLER, B. – ANDERSON, W. – CATCHPOLE, E.: *Influence of slope on fire spread rate*: In: The fire environment–innovations, management, and policy; 2007: pp. 75–82.

[9] DZIUK, G.: *Discrete anisotropic curve shortening flow*: SIAM Journal on Numerical Analysis: 36 (1999): pp. 1808–1830.

[10] FINNEY, M. A. E. A.: *FARSITE, Fire Area Simulator–model development and evaluation*: vol. 3: US Department of Agriculture, Forest Service, RMRS Ogden, UT: 1998.

[11] HOU, T. Y. – KLAPPER, I. – SI, H.: *Removing the stiffness of curvature in computing 3-d filaments*: Journal of Computational Physics: 143 (1998): pp. 628–664.

[12] HOU, T. Y. – LOWENGRUB, J. S. – SHELLEY, M. J.: *Removing the stiffness from interfacial flows with surface tension*: Journal of Computational Physics: 114 (1994): pp. 312–338.

[13] KRASNOW, K. – SCHOENNAGEL, T. – VEBLEN, T. T.: *Forest fuel mapping and evaluation of LANDFIRE fuel maps in Boulder County, Colorado, USA*: Forest Ecology and Management: 257 (2009): pp. 1603–1612.

[14] MIKULA, K. – OHLBERGER, M.: *A new level set method for motion in normal direction based on a semi-implicit forward-backward diffusion approach*: SIAM Journal on Scientific Computing: 32 (2010): pp. 1527–1544.

[15] MIKULA, K. – OHLBERGER, M. – URBÁN, J.: *Inflow-implicit/outflow-explicit finite volume methods for solving advection equations*: Applied Numerical Mathematics: 85 (2014): pp. 16–37.

[16] MIKULA, K. – ŠEVČOVIČ, D.: *Evolution of plane curves driven by a nonlinear function of curvature and anisotropy*: SIAM J. on Applied Mathematics: 61 (2001): pp. 1473–1501.

[17] MIKULA, K. – ŠEVČOVIČ, D.: *Computational and qualitative aspects of evolution of curves driven by curvature and external force*: Computing and Visualization in Science: 6 (2004): pp. 211–225.

[18] MIKULA, K. – ŠEVČOVIČ, D.: *A direct method for solving an anisotropic mean curvature flow of plane curves with an external force*: Mathematical Methods in the Applied Sciences: 27 (2004): pp. 1545–1565.

[19] MIKULA, K. – ŠEVČOVIČ, D.: *Evolution of curves on a surface driven by the geodesic curvature and external force*: Applicable Analysis: 85 (2006): pp. 345–362.

[20] MIKULA, K. – URBÁN, J.: *New fast and stable lagrangean method for image segmentation*: In: Image and Signal Processing (CISP), 2012 5th International Congress on: IEEE: 2012: pp. 688–696.

[21] MIKULA, K. – URBÁN, J.: *A new tangentially stabilized 3D curve evolution algorithm and its application in virtual colonoscopy*: Advances in Computational Mathematics: 40 (2014): pp. 819–837.

[22] OSHER, S. – FEDKIW, R.: *Level Set Methods and Dynamic Implicit Surfaces*: Applied Mathematical Sciences: Springer New York: 2002.

[23] PAUŠ, P. – BENEŠ, M.: *Algorithm for topological changes of parametrically described curves*: In: Proceedings of ALGORITMY: 2009: pp. 176–184.

[24] PRICHARD, S. J. ET AL.: *Fuel characteristic classification system version 3.0: Technical documentation*: tech. rep.: U.S. Department of Agriculture, Forest Service, PNRS: 2013.

[25] SCOTT, J. H. – BURGAN, R. E.: *Standard fire behavior fuel models: a comprehensive set for use with rothermel's surface fire spread model*: The Bark Beetles, Fuels, and Fire Bibliography: (2005): p. 66.

[26] SETHIAN, J. A.: *Level set methods and fast marching methods: evolving interfaces in computational geometry, fluid mechanics, computer vision, and materials science*: Cambridge university press: 1999.

[27] SULLIVAN, A.: *A review of wildland fire spread modelling, 1990-present 3: Mathematical analogues and simulation models*: arXiv preprint arXiv:0706.4130: (2007).

[28] VIEGAS, D. ET AL.: *Slope and wind effects on fire spread*: In: IVth International Forest Fire Conference. Coimbra (Portugal). FFR & Wildland Fire Safety. Millpress, Rotterdam.: 2002.

List of author's publications

1. AMBROZ, M. – BALAŽOVJECH, M. – MEDĽA, M. – MIKULA, K.: *Numerical modeling of wildland surface fire propagation by evolving surface curves*. Manuscript submitted for publication.

2. AMBROZ, M. – BALAŽOVJECH, M. – MIKULA, K.: *Mathematical model of forest fires propagation*. In Advances in architectural, civil and environmental engineering [elektronický zdroj] : 25rd Annual PhD Student Conference on Architecture and Construction Engineering, Building Materials, Structural Engineering, Water and Environmental Engineering, Transportation Engineering, Surveying, Geodesy, and Applied Mathematics. Bratislava, SR, 28. 10. 2015. Bratislava : STU v Bratislave, 2015, CD-ROM, s. 13-19. ISBN 978-80-227-4514-7.

3. AMBROZ, M. – MIKULA, K.: *Surface curve as a fire border*. In Advances in Architectural, Civil and Environmental Engineering [elektronický zdroj] : 26th Annual PhD Student Conference on Architecture and Construction Engineering, Building Materials, Structural Engineering, Water and Environmental Engineering, Transportation Engineering, Surveying, Geodesy, and Applied Mathematics. 26. October 2016, Bratislava. Bratislava : STU v Bratislave, 2016, CD-ROM, s. 13-19. ISBN 978-80-227-4645-8.

4. AMBROZ, M. – MIKULA, K.: *Asymptotically uniform redistribution of a curve points on a surface*. In Advances in Architectural, Civil and Environmental Engineering [elektronický zdroj] : 27th Annual PhD Student Conference on Applied Mathematics, Applied Mechanics, Geodesy and Cartography, Landscaping, Building Technology, Theory and Structures of Buildings, Theory and Structures of Civil Engineering Works, Theory and Environmental Technology of Buildings, Water Resources Engineering. 25. October 2017, Bratislava, Slovakia. Bratislava : Spektrum STU, 2017, CD-ROM, s. 14-19. ISBN 978-80-227-4751-6.